OPTIMISATION OF WIDEBAND SINUOUS ANTENNA PARAMETERS FOR ULTRA-WIDEBAND APPLICATIONS

Hong Hung Leung[1], Sng Yi Xin[2], Huang Ying Ying[3], Lim Zi Wei[3]
[1]Dunman Secondary School, 21 Tampines Street 45, Singapore 529093
[2]Singapore Chinese Girls' School, 190 Dunearn Road, Singapore 309437
[3]DSO National Laboratories, 12 Science Park Drive Singapore 118225

ABSTRACT

Sinuous antennas are used in applications such as radar and direction-finding systems due to their ultra-wideband (UWB) frequency capabilities. However, they tend to suffer from performance-degrading resonances, leading to uneven gain and distorted radiation patterns that occur log-periodically and at the ends of the antenna. Current solutions involve some form of truncation or additional modification to the antenna trace, which damages its self-complementary structure. We propose a novel approach to optimising the parameters used to generate sinuous traces so as to counteract such resonances and to provide better bandwidth and gain as compared to a traditional sinuous antenna, negating the need for additional modification wield decreasing antenna size. Proposed changes are simulated using Ansys HFSS, and verified through measurement in an anechoic chamber with an operating bandwidth of 1-6 GHz.

INTRODUCTION

Sinuous antennas are frequency-independent antennas. Frequency independent antennas follow Rumsey's principle, which states that the impedance and pattern properties of an antenna will be frequency-independent if the geometry of the antenna satisfies the scale principle, where its geometry can be specified entirely in terms of angles, and is therefore independent of a change of scale of an antenna [1]. The highest operating frequency of such an antenna occurs when the shortest dipole is nearly λ/2, and its lowest frequency is determined by the λ/2 length of the longest element [2].

A sinuous antenna is a combination of a log-periodic antenna and a spiral antenna. The sinuous antenna was first published in a patent by DuHamel in 1987 [3]. A sinuous antenna works in a manner similar to a spiral antenna: current enters the antenna through the feed points from the centre of the antenna, where there is one feed point per arm. The current will travel along the sinuous curves until it reaches the region on an arm that corresponds to λ/2, where it will form a "ring" around the circumference of the corresponding arms. This is also known as the *band theory* or *radiating ring theory* [4]. Most residual current attenuates away before it can excite the next active region. Figure 1 is an example of a sinuous antenna.

Figure 1: Example of four-armed sinuous antenna

Sinuous antennas have a low-profile planar structure, and unlike other low-profile frequency independent antennas, such as spiral antennas and log-periodic antennas, require no

additional modifications, either geometrically or to the feed structures, in order to achieve dual polarisation. Sinuous antennas are also capable of circular polarisation with the addition of a hybrid coupler, which generates a phrase difference of 90° between the horizontally and vertically polarised arms, allowing the antenna to achieve either Left-Hand or Right-Hand Circular Polarisation (LHCP and RHCP), depending on how the arm pair is fed.

The impedance and pattern properties of the antenna generally remain consistent throughout the various frequencies, making them frequency-independent. This is unlike regular antennas, where the radiation pattern, impedance, and gain change with the frequency of the antenna. Since the impedance and pattern properties of sinuous antennas is independent of a change of frequency, frequency independent antennas typically have wider frequency ranges. This allows frequency independent antennas to achieve ultra-wideband (UWB) radiation, making them suitable for use in systems that require UWB antennas such as direction-finding and radar systems.

Whilst there has been extensive research on sinuous antennas, past research on improving the performance of the antenna had mainly revolved around the truncation of traces in order to reduce resonance and improve performance. However, research on optimising the parameters used to generate the antenna is lacking. Though the effects of changing these parameters has been somewhat explored, no other authors have attempted to optimise them as a solution to resonances and poor gain in themselves without additional modifications. Hence, our study aims to better determine the effect of optimising antenna parameters, uniformly and with variation within traces. In addition, we will also attempt truncation to improve antenna performance, as explored in some previous studies [4][5][6], and compare it to our proposal.

MATERIALS AND METHODS

$$\phi = (-1)^p \alpha \sin\left(\frac{\pi \ln\left(\frac{r}{R_p}\right)}{\ln(\tau)}\right) \pm \delta \quad (1)$$

$$x = R_{inner}\cos(u), y = R_{inner}\sin(u) \quad (2)$$

$$x = R_p\cos(u), y = R_p\sin(u) \quad (3)$$

Sinuous antennas consist of p number of cells, and are drawn following equations (1) - (3), where **α** is the angular width of each cell, **τ** is the decay factor of successive cells, and **δ** determines the angular thickness of the trace. A larger value of **τ** would result in thinner and finer traces, while larger values of **α** result in thinner traces with more interleaving. These effects are demonstrated in Figures 3 and 8, where we vary values of **τ** and **α** to investigate their impact. In most sinuous antennas, **τ** and **α** are kept constant throughout the antenna. Equation (1) describes a single cell in polar coordinates, while parametric equations (2) and (3) describe arcs used to close off the inner and outer radii of the arms. Following this, equations (4) and (5) are used to determine the inner and outer radii of the trace. Figure 2 demonstrates the generation process.

$$R_{inner} = \frac{\lambda_{upper}}{4(\alpha_p + \delta)} \quad (4)$$

$$R_{outer} = \frac{\lambda_{lower}}{4(\alpha_p + \delta)} \quad (5)$$

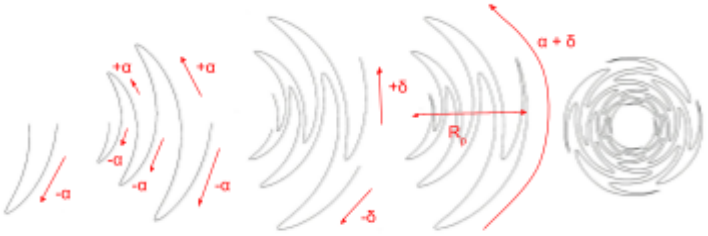

Figure 2: Process of generating a sinuous trace

Truncating the antenna suddenly can lead to distorted radiation patterns due to the reflection of current at the outer ends, or interference from feeding regions in the inner ends, antennas tend to extend beyond the dimensions calculated in (4) and (5). (4) is usually halved to account for this.

For the purposes of this project, we investigate an antenna with 4 arms and **δ** value of 22.5°. Sinuous antennas with 6 or 8 arms do exist, and are usually used due to beamformer limitations and to achieve additional modes [4]. We chose to improve upon the general design of a 4-armed sinuous antenna. As our variables are parametric, they should be applicable to any sinuous antenna drawn with equations (1) - (3).

To investigate the effects of varying constant **τ**, four antennas with a radius of 2.5 cm were simulated with values of **τ** = 0.6, **τ** = 0.7, **τ** = 0.8, and **τ** = 0.9 (Figures 3a - 3d, left to right), while **α** was kept constant at 45°, the results of which are shown in Figure 4. Note that the inner radius of the antennas increases quickly with **τ**, which degrades high-frequency performance as outlined in (4), so high-frequency gain between these simulations is not strictly comparable. It was observed that higher values of **τ** lead to better low-frequency performance, which would be expected from (5), and more surprisingly, that higher values of **τ** result in less gain loss as frequency becomes lower than the value predicted in equation (5). Gain values remain relatively smooth for values of **τ** = 0.6, **τ** = 0.7, **τ** = 0.8, with large resonances observed in the antenna with a **τ** value of 0.9. This is due to interleaving between arms: while interleaving allows for the radiating ring effect to take place, excessive interleaving can cause interference and decreases in gain due to mutual coupling between arms.

Figure 3a: τ = 0.6

Figure 3b: τ = 0.7

Figure 3c: τ = 0.8

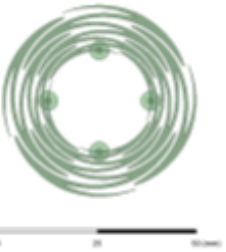

Figure 3d: τ = 0.9

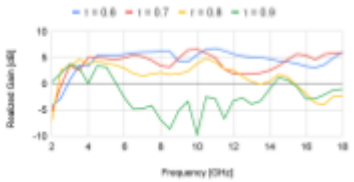

Figure 4: Effect of varying τ

In order to benefit from the better gain in low frequencies that higher values of **τ** provided, prototypes of radius 5.0 cm were designed with **τ** decreasing towards the centre of the antenna (Figure 5). Simulated antenna have 20 cells per trace with values of **τ** = 0.9 for the outermost 10 cells (cells 1-10), **τ** = 0.875 for the next 5 cells (cells 11-15), **τ** = 0.85 for cells 16-17, and **τ** = 0.8 for cells 18-20 unless otherwise stated. This enables the outermost cells, which are excited in low frequencies, to have higher values of **τ**, allowing for better gain in low frequencies. Lower values of **τ** towards the centre of the antenna

prevent the effects of excessive interleaving. To investigate any differences in performance due to this variation, a variant of the final design where **τ** is kept constant at **τ** = 0.9, is simulated and compared to simulations of an antenna with **τ** variation (Figure 6). Note that the range of frequencies simulated in Figure 4 is 2-18 GHz, while the range of frequencies in Figure 6 is 1-9 GHz. This is due to an increase in the outer radius from 2.5 cm to 5.0 cm, for ease of fabrication. Due to the frequency-independent nature of sinuous antennas, this change does not affect the validity of the results.

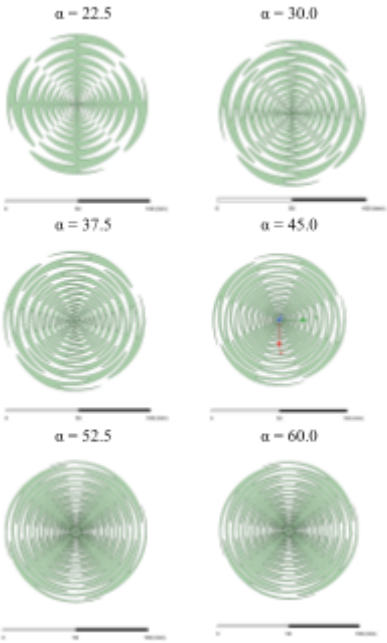

Figure 5: Effects of α on traces

Figure 6: Effect of varying τ

Different values of **α** were then simulated to determine its effects on antenna performance (Figure 7). As seen in Figure 5, increasing **α** increases the amount of interleaving between traces, with **α** < 22.5° (**α** < **δ**) having no interleaving. Simulations show that though the antenna of **α** = 22.5° had the highest average gain, due to the lack of interference from interleaving, it did not perform well in lower frequencies, with gain being both low and inconsistent from 1 - 3.25 GHz. The other simulations had similar gain on average, with gain in lower frequencies improving as **α** increased. Figure 7 shows gain from **α** = 22.5°, **α** = 45.0°, and **α** = 60.0°, while Figure 8 shows gain for all 6 antennas in frequencies <1.5 GHz.

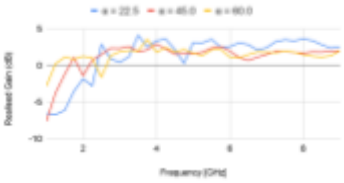

Figure 7: Effect of α

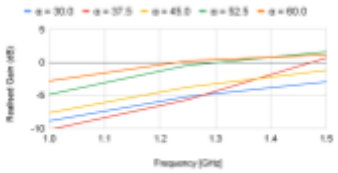

Figure 8: Effects of α, <1.5 GHz

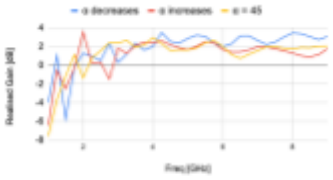

Figure 9: Effect of varying α

For the final design, **α** was decreased from the outer radius to the centre of the antenna, so that the largest values of **α** were located on the outer radius while the smallest were located on the inside radius. This was to benefit from the better low-frequency gain caused by higher values of **α** on the outer cells, while inner cells have lower values of **α** to prevent interference due to excessive interleaving, and to keep traces thick enough to fabricate. To verify this, an antenna where **α** decreases linearly (from the outside radius inwards) from 60° and 22.5° was simulated, and compared it to antennas where **α** remains constant at 45° and where **α** increases linearly from 22.5° to 60°, the results of which are shown in Figure 9. It is clear that decreasing values of **α** led to better gain in high and low frequencies, as higher interleaving in the outer cells allows for better low-frequency gain, while lower interleaving towards the centre prevents interference. However, interference was still observed at 1.5 GHz, so values of **α** were further adjusted through equation (6)

$$-\boldsymbol{\sigma} log(p) + \alpha_{initial} \quad (6)$$

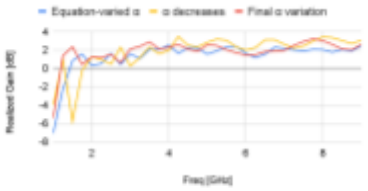

Figure 10: Methods of varying α

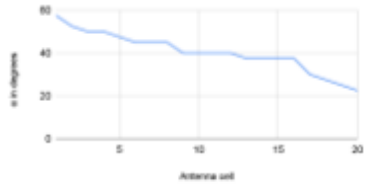

Figure 11: Final variation of α

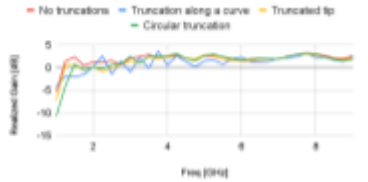

Figure 12: Effects of truncation

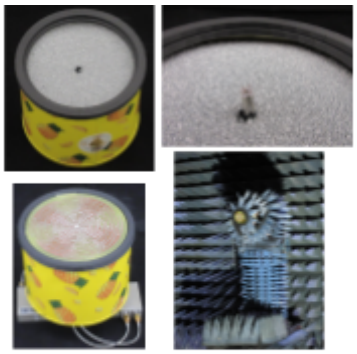

Figure 13 (clockwise, starting at top left): Metal container with absorbers and mount, close up of wires, complete antenna, and measurement taking place in an anechoic chamber.

Where σ is a variable, p is the nth sinuous trace and $\alpha_{initial}$ is the initial value of α. For our simulations, σ = 17.5 and $\alpha_{initial}$ = 55°. When a line is drawn connecting the tips of the antenna traces, this will form a curve from the centre to the tip of the last antenna trace, allowing for α to decrease faster, decreasing interference. Figure 10 compares this antenna to one where α varies linearly downwards. While interference was reduced, varying α with the equation negatively affected higher frequencies, as α decreased more slowly after the first few cells, leading to a higher α value towards the centre, causing more interleaving and interference. Hence, we modified α in our final design to vary in three distinct sections: a steep decrease in the outer cells, a slower decrease in the middle cells, and another steep decrease in the innermost section. As seen in Figure 10, this leads to better gain as compared to varying α with the equation, and more consistent gain than linearly varied α. Figure 11 shows the values of α used, with the exact values provided in Appendix 2.

Truncating the final design was attempted as detailed in [5] and [7]. Truncation along a curved line was also attempted. Figure 12 shows the results of these simulations, while Appendix 3 shows details of truncations according to past studies. As we did not observe any substantial improvement in gain, truncation was not implemented in the final prototype design.

To fabricate the finalised prototype, absorbers were placed in a cylindrical metal container with a similar diameter to the antenna. This is because sinuous antennas produce two lobes of radiation, only the forward-facing one of which is desired. Cables were connected to the balun below the cylinder. Finally, a mount for the antenna was printed using a Markforged 3D printer. The antenna was then tested in an anechoic chamber across the frequencies of 1-6 GHz. Figure 13 shows the fabricated antenna and the measurement process.

The plotting and simulation of traces was carried out on HFSS through Ansys Electronics Desktop. The design was then exported to Solidworks where it was modelled before being printed by an LPKF PCB milling machine. The chosen design was printed on 60 mil Rogers 4350b substrate, while the traces themselves were made of copper. The coaxial cable used is product no. 1617B manufactured by Belden Inc. with a conductor of silvered copper with a diameter of approximately 0.05mm. The coaxial cable was cut and stripped manually through the usage of wire-stripping tools, and SubMiniature Version A (SMA) connectors were then soldered onto the cable. The coaxial cable was then attached to a balun with an operating frequency of 1-12GHz.

RESULTS

The prototype design was simulated and results were compared to measurements. We can see that gain is even better than expected from simulated results, particularly in low frequencies. Figure 14 shows the simulated results and measurements in the E and H planes, measured by exciting the vertical (V port) and horizontal (H port) ports respectively. Figures 15 and 16 show the simulated radiation pattern and measured radiation patterns respectively, in co-polarisation (co-pol). Variation is observed as frequency increases, with some smaller lobes observed alongside the larger main lobe. Figure 17 shows return loss of the antenna from 1-9 GHz, showing good impedance matching as S11, S22, S33, and S44 remain below -10dB from 4 GHz - 9 GHz, and below -5dB for all frequencies.

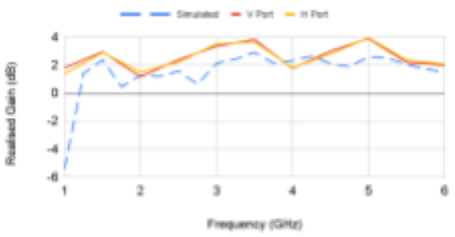

Figure 14: Simulated and measured gain

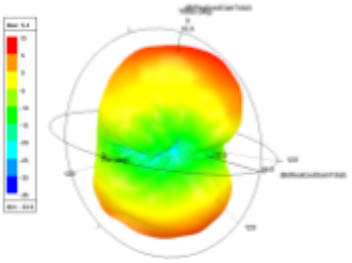

Figure 15a: 3D radiation pattern

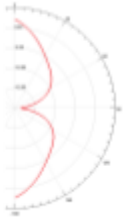

Figure 15b: 2D radiation pattern, showing front and back lobes

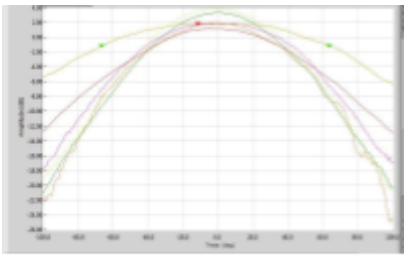

Figure 16a: Co-pol realised gain, V Port, E-plane

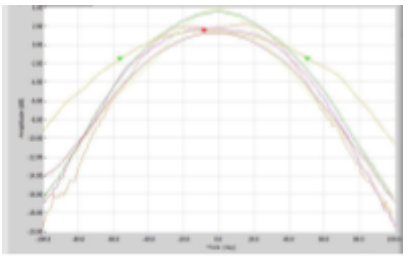

Figure 16b: Co-pol realised gain, V Port, H-plane

A	FF Tx [deg]	Freq. [GHz]	Phi [deg]
	90.00	1.000 G	90.00
	90.00	2.000 G	90.00
	90.00	3.000 G	90.00
	90.00	4.000 G	90.00
	90.00	5.000 G	90.00

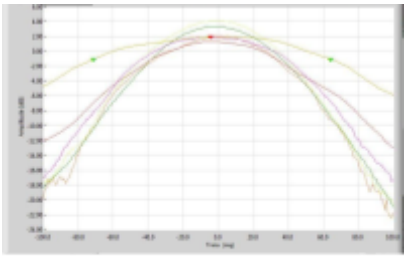

Figure 16c: Co-pol realised gain, H Port, E-plane

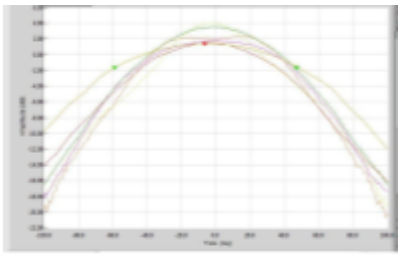

Figure 16d: Co-pol realised gain, H Port, H-plane

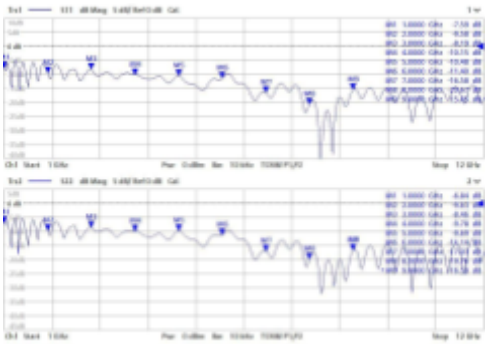

Figure 17a: S11 and S22

Figure 17b: S33 and S44

DISCUSSION

The results show that the prototype functions well across a range of 1-6 GHz, and as measurements correspond well with simulations, the antenna should work as intended within the simulated frequencies of 1-9 GHz. Gain is markedly more consistent than antennas simulated without optimisation of α and τ (Figures 4, 6, 9, and 10), with lessened log-periodic resonances and greatly improved low-frequency gain. Furthermore, gain at the lowest frequencies was greatly increased, which was surprising as equation (5) shows that a sinuous antenna operating at 1 GHz should require, at minimum, an antenna 5.36 cm in radius. Given that the radius is often larger than the value given in (5) so as to prevent reflection of current, our proposal has been effective in increasing bandwidth and gain without enlarging the antenna, and could also be used to reduce antenna size without compromising bandwidth.

Further optimisation could be carried out based on our findings, with more research into improving bandwidth and gain through optimisation of parameters, rather than additional modifications. Truncation was observed to have little positive effect on our optimised design. This is likely due to truncation effectively reducing angular width α, causing less interleaving at the cost of lower bandwidth. Before optimisation of antenna parameters, reducing interleaving improved gain as seen in Figure 4. However, after our suggested improvements, reducing interleaving through truncation is not beneficial as interleaving had already been controlled through variations in α and τ.

LIMITATIONS AND FURTHER WORK

Sinuous antennas are capable of radiating in higher modes than the lowest mode investigated in this report, especially in antennas with more than 4 arms, or in conical and pyramidal antennas [4]. Further work may be carried out on whether varying α and τ has similar effects on 6 and 8-armed sinuous antenna. Though α and τ are part of the general equation used to draw any sinuous antenna, and should have a predictable effect regardless of the specific antenna drawn, 6 and 8-armed sinuous antenna support higher modes of radiation than the 4-armed antenna investigated here, and hence the effects of our changes to α and τ on these higher modes is unknown.

It has been demonstrated that the electrical permeability of the antenna substrate affects its gain and its lowest operating frequency, as substrates of a higher dielectric constant allow a lower minimum operating frequency but also lower gain [8]. More research on this area could be carried out. This was also a limitation of our study, as we did not investigate the substrate, which may account for the differences between our simulations and measurements.

CONCLUSION

This project shows that through optimised variations of α and τ, the gain and bandwidth of a sinuous antenna can be greatly improved without truncation or other modifications to the antenna structure. We discuss the reasoning and process of selecting α and τ values, and how

our improvements upon sinuous antenna design help to mitigate unwanted resonances and interference, while improving gain, gain consistency, and bandwidth.

ACKNOWLEDGEMENTS

We would like to thank our mentors, Huang Ying Ying and Lim Zi Wei, for guiding us throughout this project, as well as everyone in our lab and the DSO EN Division for helping us along the way.

REFERENCES

[1] V. Rumsey, "Frequency independent antennas," 1958 IRE International Convention Record, 1957, pp. 114-118, doi: 10.1109/IRECON.1957.1150565.

[2] Kubacki, R.; Czyżewski, M.; Laskowski, D. Enlarged Frequency Bandwidth of Truncated Log-Periodic Dipole Array Antenna. Electronics 2020, 9, 1300. https://doi.org/10.3390/electronics9081300

[3] R. H. Duhamel, “Dual Polarized Sinuous Antennas,” U.S. Patent 4658262, 1987.

[4] Volakis, J. L. (2019). *Antenna Engineering Handbook* (4th ed.). McGraw Hill Education.

[5] D. A. Crocker and W. R. Scott, "Sinuous Antenna Design for UWB Radar," 2019 IEEE International Symposium on Antennas and Propagation and USNC-URSI Radio Science Meeting, 2019, pp. 1915-1916, doi: 10.1109/APUSNCURSINRSM.2019.8888630.

[6] Sammeta, R. 2014. Low-Profile Antennas for Wideband Transmit Application in HF/UHF Bands.

[7] D. A. Crocker and W. R. Scott, "On the Design of Sinuous Antennas for UWB Radar Applications," in IEEE Antennas and Wireless Propagation Letters, vol. 18, no. 7, pp. 1347-1351, July 2019, doi: 10.1109/LAWP.2019.2916477.

[8] P. Baldonero, A. Manna, F. Trotta, A. Pantano and M. Bartocci, "UWB Double polarised phased array," 2009 3rd European Conference on Antennas and Propagation, 2009, pp. 556-560.

APPENDIX 1

Exploration of alternative antennas for UWB applications

Other types of UWB antennas, such as Vivaldi antennas, are also capable of radiating and receiving signals across a large bandwidth. Both antennas can achieve dual polarisation [9], and circular polarisation [10], allowing it to be more accurate when used in applications such as direction finding systems. Another key similarity between Vivaldi and Sinuous antennas is that they are both frequency independent antennas, allowing the Vivaldi antenna to operate with high gain and stable beamwidth [11]. Figure 18 shows a Vivaldi antenna.

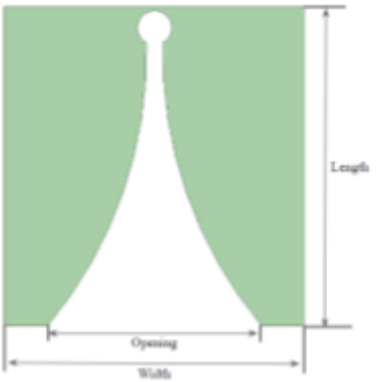

Figure 2: Vivaldi antenna

Despite their similarities, sinuous antennas have some significant advantages over Vivaldi antennas. A key difference which makes sinuous antennas more practical than a Vivaldi antenna is their difference in size. Though sinuous antennas and Vivaldi antennas could theoretically have the same operating bandwidth and similar gain, the size of Vivaldi antennas increases more as the lowest frequency in the antenna's operating frequency decreases. A Vivaldi antenna with a lowest frequency of 2 GHz would require an opening of at least 7.5 cm wide, while a sinuous antenna would have a radius of 2.68 cm (which can be reduced further, as shown by our report). Furthermore, this does not take into account the length of the Vivaldi antenna, which would be longer than its width. In addition, Vivaldi antennas can achieve dual and circular polarisation but this can only be done with a 3D structure consisting of 4 Vivaldi elements, 2 coplanar horizontal and 2 coplanar vertical elements which further increases the size of the Vivaldi antenna. In contrast, a sinuous antenna is planar, with the only 3D components being absorbers (to absorb back-lobe radiation) and balun.

Many applications of the sinuous antenna, such as military applications prefer low-profile and lightweight antennas for portability, and civil applications such as radar systems that require UWB radiation also usually prefer low profile antennas for aesthetic purposes. Therefore, due to the larger (or significantly larger, for applications that require dual or circular polarisation) size of Vivaldi antennas as compared to sinuous antennas, sinuous antennas are preferred in UWB applications.

[9] Sun,H.-H., Lee,Y.H., Luo, W., Ow, L.F., Yusof, M.L.M., Yucel, A.C., Compact Dual-Polarized Vivaldi Antenna with High Gain and High Polarization Purity for GPR Applications. Sensors 2021, 21, 503. https://doi.org/10.3390/s21020503

[10] Ren, X., Liao, S., & Xue, Q. (2018). Design of wideband circularly polarized Vivaldi antenna with stable radiation pattern. *IEEE Access*, *6*, 637–644. https://doi.org/10.1109/access.2017.2773566

[11] Borda Fortuny, C., Tong, K. F., Chetty, K., & Benton, D. M. (2014). High-gain frequency reconfigurable Vivaldi antenna. *2014 IEEE Antennas and Propagation Society International Symposium (APSURSI)*. https://doi.org/10.1109/aps.2014.6904953

APPENDIX 2

Cell	1	2	3-4	5	6-8	9-12	13-16	17	18	19	20
α	57.5°	52.5°	50.0°	47.5°	45.0°	40.0°	37.5°	30.0°	27.5°	25.0°	22.5°

APPENDIX 3

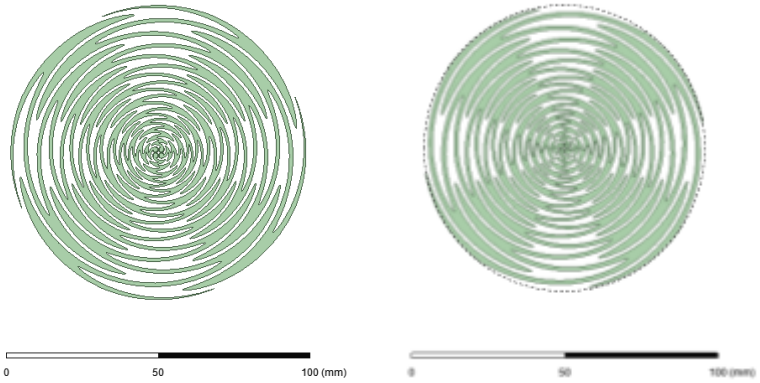

Left: Antenna without truncations. Right: Circularly truncated antenna.

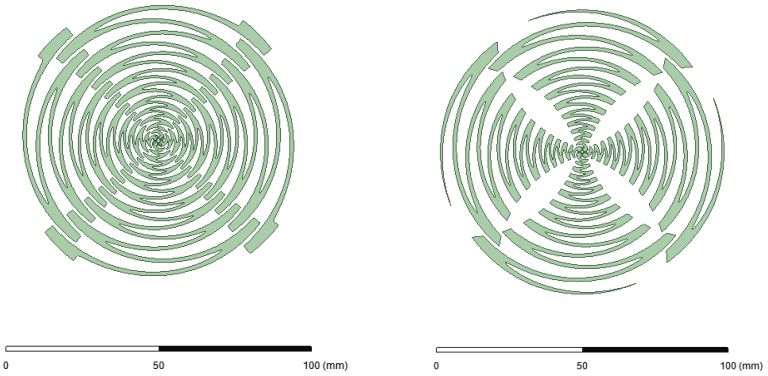

Left: Straight truncation. Right: Truncation along a curve.

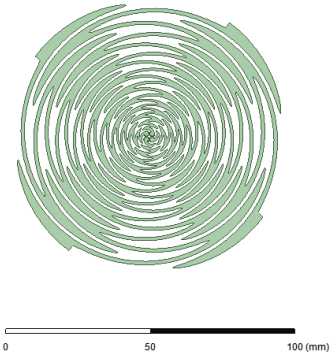

Truncation of antenna tip.